AIMS Materials Science, 10(2): 288–300.
DOI: 10.3934/matersci.2023015
Received: 03 October 2022
Revised: 21 January 2023
Accepted: 07 February 2023
Published: 28 February 2023

http://www.aimspress.com/journal/Materials

Research article

Low-cost piezoelectric sensors and gamma ray attenuation fabricated from novel polymeric nanocomposites

Shaimaa Mazhar Mahdi and Majeed Ali Habeeb*

University of Babylon, College of Education for Pure Sciences, Department of Physics, Iraq

* **Correspondence:** Email: pure.majeed.ali@uobabylon.edu.iq.

Abstract: This study looks at the synthesis of innovative PEO/PVA/$SrTiO_3$/NiO nanocomposites for piezoelectric sensors and gamma shielding applications that are low weight, elastic, affordable and have good gamma ray attenuation coefficients. The impact of $SrTiO_3$/NiO on the structural characteristics of the PEO/PVA mixture is investigated. The polymer mixture PEO/PVA received additions of $SrTiO_3$/NiO at concentrations of (0, 1, 2, 3 and 4) weight percent by the casting method. On the top surface of the films PEO/PVA/$SrTiO_3$/NiO NCs, scanning electron microscopy reveals several randomly distributed aggregates or fragments that are consistent and coherent. An optical microscope image collection reveals that the blend's additive distribution of NPs was homogenous. Gamma ray shielding application results show that the attenuation coefficient of PVA/PEO/$SrTiO_3$/NiO NCs is increased by increasing concentration of $SrTiO_3$/NiO nanoparticles. Radiation protection is another application for it. The pressure sensor application findings of NCs show that, when the applied pressure rises, electrical capacitance (Cp) increase.

Keywords: nanocomposites; $SrTiO_3$/CoO NPs; piezoelectric sensors; gamma ray attenuation

1. Introduction

The manufacturing of novel polymer nanocomposites has been extensively researched in recent years in the sectors of barrier fields, coatings, antibacterial, sensors, antiballistic goods, conductive and other materials. The sort of the additive the polymer matrix uses has an impact on nanoparticles. The applications include a wide range of industries, such as electronics, aircraft, the military, transportation and medical [1,2]. With only one polymer, it is impossible to personalize the final result of the blending

process to fit the needs of the applications. Polyethylene oxide is a semi-crystalline and linear polymer (PEO). Given that polyethylene oxide is a linear polymer, a high degree of crystallinity is permitted by the regularity of the structural device. The cations of the metal salts can interact and connect with the polar group O in the chemical structure of PEO [3]. Numerous salt varieties can be resolved with PEO. However, because of the C–O, C–H and C–C bonds in its structural unit, it is chemically and electrochemically stable, and has a low level of reactivity. The high concentration of the crystalline phase, however, limits the conductivity of the polyethylene Oxide polymer [4]. One of the first, and most popular polymers, is polyvinyl alcohol (PVA), which is utilized extensively in semiconductor manufacturing today [5]. It has been shown that $SrTiO_3$ possesses persistent photoconductivity, which indicates that shining light on the crystal causes it to become more electrically conductive by one factor or more. In the last forty years, a variety of semiconductors, including $SrTiO_3$ NPs, with adequate conduction band locations and band gaps, were employed as photo catalysts to split water for the production of hydrogen [6]. Due to their high thermal and chemical stability, environmental friendliness and industrial use, nickel oxide nanoparticles NiO NPs, one of the most significant transition metal oxides, have a variety of properties when reacting with polar surface materials. When radiation particles fall on matter, the energy of these particles is gradually transmitted to matter through collisions with atoms of matter until they stop. As a result of these collisions, the atoms of the substance are ionized; that is, the electron is completely separated from its atom. The way gamma ray energy is lost varies in matter, photoelectric effect, pair production and the Compton effect. A gamma photon interacts with one of the electrons in the inner levels of the atom; with electrons in the last orbit of the atom. In this interaction, the beam is dispersed. The fallen one's direction changes, and its energy decreases [7]. X-rays and γ-rays have many applications in military, medical, health, scientific and agricultural industries. Increasing the utilization of hazardous radiations, including gamma sources in hospitals and research centers for diagnostic and therapeutic applications, has provided a more insecure place for personnel. Thus, there will be a need to design an appropriate shield [8]. Other applications of polymer nanocomposites are flexible electronics, solar cells, anti-static devices, electromagnetic interference shields, radiation shields, nuclear materials in reactors, battery electrode materials, lightweight energy storage devices, super-capacitors, piezoelectric sensors, radiation sensors, lightweight spacecraft electronics and ionizing radiation dosimeters [9–11]. Shielding of radiation is especially a crucial section in the programs of radiation protection. Typically, concrete is the general and normally used matter to the radiation shielding in mainly facilities, like hospitals. The huge available quantity and cost efficiency of concrete were its major advantages as a shielding material. However, it has several disadvantages, like the cracks that may happen after a long period of time of exposure to radiation and the difficulty of transporting it. The synthetic polymers can be employed to manufacture novel materials, and may be used to make a radiation shielding. Furthermore, their additional advantages, like durability, low industrialized cost and high chemical and thermal stability, are amid the preferential traits and quality used for greater shielding [12]. Different researchers have studied pressure sensors and gamma shielding. Shirinov et al. [13] studied a piezoelectric polyvinyl lidene fluoride (PVDF) film. The properties of the sensor have been experimentally investigated. The cross-sensitivity to temperature and humidity, and the response time were measured. They found that the capacitance of film increased as pressure increased. Janczak et al. [14] studied the characteristics of PMMA/PVDF/Gr nanocomposites. They showed that the relationship between resistance and pressure is nearly linear on a logarithmic scale for selected types of samples, and their response is several times higher than for similar sensors with graphite layers. Gavrish et al. [15] found an

improvement in thermo physical, radiation-shielding and mechanical properties by varying the amount of tungsten nanopowder. $Bi_2O_3$was dispersed in Bi_2O_3/XNBR films, in the concentration range of 30–70 wt% by Liao et al. [16], where these samples had an effective role in attenuating low energy gamma rays. Abdalsalam et al. [17] showed that; samples were fabricated by adding 0.5, 1, 1.5, and 2 wt% of Bi_2O_3 into ultra-high molecular weight polyethylene, and then using a hot-press. The results of this study indicated that the measurements of (μ/ρ) for energies between 30.8 and 383.9 keV showed that the specimen with 2 wt% Bi_2O_3 exhibited the highest photon attenuation. This work aims to prepare and characterize PEO/PVA/$SrTiO_3$/NiO nanocomposites for pressure sensors and gamma ray attenuation.

2. Materials and methods

In this work, nanocomposites were created by combining (PEO/PVA) in 40 mL distilled water with a magnetic stirrer at 70 ℃ for 45 min to produce a more uniform solution. The addition of ($SrTiO_3$/NiO) NP with concentrations 0, 1, 2, 3, and 4 wt% followed the casting method (Figure 1). The samples were tested at different concentrations by using an Olympus type Nikon-73346 optical microscope, which has a magnifying power of (10×) and is equipped with a camera used in the microscopic photography. A scanning electron microscope was used for the surface morphology of (PEO/PVA) and ($SrTiO_3$/NiO) NCs. Dual Broker Flash EDS detectors and Broker flash HD EBSD (Czech Tuscan Instrument Co.) were included in the Tuscan Mira3 SEM microscope for analytical issues. Using nanocomposites for gamma ray shielding, the gamma-ray attenuation characteristics for volume fractions changing concentrations of ($SrTiO_3$/NiO) nanoparticles have been studied. Samples were positioned in front of a collimated beam coming from gamma ray sources (Cs-137.5 mci). The distance between the gamma ray and the detector was two centimeters. The linear attenuation coefficients were calculated using Geiger counter measurements of transmitted gamma ray fluxes via nanocomposites made of PEO/PVA/$SrTiO_3$/NiO NCs. The usefulness of the pressure sensor NCs was assessed by calculating the parallel capacitance between the two poles above and below the specimen using the LCR matrix for various pressure ranges (80–160 bar).

The following Eq 1 may be used to get the linear attenuation coefficients (μ) from the thicknesses of the material [18,19]:

$$N=N_o\, e^{-\mu x} \tag{1}$$

where N_o is a gamma ray incident, N is the attenuation of the gamma rays and x is the thickness of the sample.

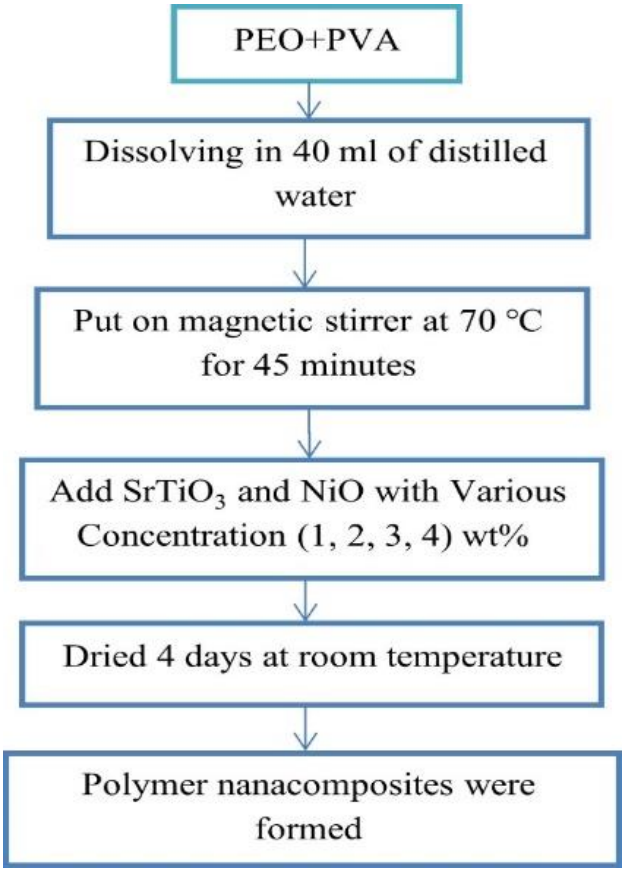

Figure 1. Schematic illustration of the synthesizing process of the nanocomposites.

3. Results and discussion

3.1. Scanning electron microscope (SEM) measurements of PEO/PVA/ $SrTiO_3$/NiO NCs

The whole impact of $SrTiO_3$/NiO nanoparticle concentration is investigated, and the dispersion of nanocomposites particles in the polymer matrix is examined using a scanning electron microscope. Figure 2 depicts a SEM micrograph of pure blend surface for films made of PEO/PVA /$SrTiO_3$/NiO NCs, which were applied one after the other with varying amounts of $SrTiO_3$/NiO nanoparticles. For polymer blend, image (a) in Figure 2 is found to be transparent, correlated and has a consistent shape, which reveals a rather soft surface. The surface morphology of the polymer blends PEO/PVA $SrTiO_3$/NiO in Figure 2a,c changes with increasing nanoparticle ratios. Nanocomposites films exhibit numerous spherical particle aggregates or chunks that are evenly dispersed, and widely spaced on the surface. This could be a sign of a homogeneous growth mechanism [20–22]. Surface morphology varies as the nanoparticle ratio in polymer blends rises, see Figure 2c. When the $SrTiO_3$/NiO NCs rise, the grain clumps. The results would show the PEO/PVA/$SrTiO_3$/NiO membranes' surface morphology. As the concentration of $SrTiO_3$/NiO NCs increases, more aggregates or fragments are randomly distributed on the upper surface of nanoparticles [23,24].

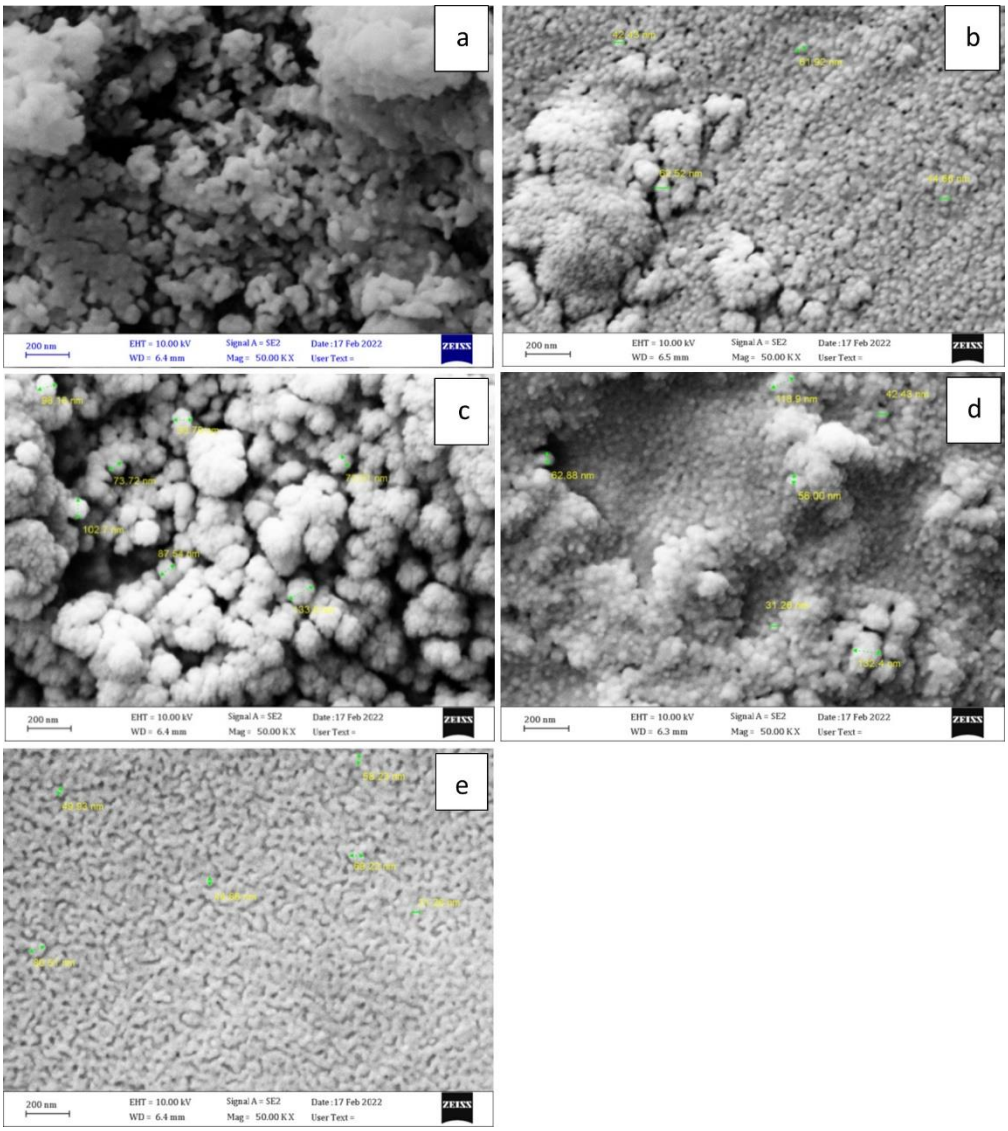

Figure 2. SEM for PEO/PVA/$SrTiO_3$/NiO NCs are shown in (a) for PEO/PVA, (b) for 1 wt% $SrTiO_3$/NiO, (c) for 2 wt% $SrTiO_3$/NiO, (d) for 3 wt% $SrTiO_3$/NiO and (e) for 4 wt% $SrTiO_3$/NiO.

3.2. Optical microscope for PEO/PVA/$SrTiO_3$/NiO NCs

Figure 3 shows cross-sectional photomicrographs of PEO/PVA/$SrTiO_3$/NiO nanocomposites at a power of 10× magnification. It was discovered that the $SrTiO_3$/NiO nanoparticles and the PEO/PVA mixture could be readily distinguished in the nanocomposites. The $SrTiO_3$/NiO nanoparticles exhibit an annularly linked network in the PEO/PVA matrix, which is caused by the filler's sponge-like form. This indicates that the nanoparticles fill the matrix in a regular three-dimensional manner. The PEO/PVA mixture completely filled the interspace of the $SrTiO_3$/NiO nanoparticle sponges, and, based on the detailed photomicrographs in Figure 3, there is a clear distinction from the tests [25]. This is shown by the good contacts between the $SrTiO_3$/NiO nanoparticle structure and blend matrix without any obvious cracks or pores. In nanocomposites, the shape can be distinguished clearly. Nanoparticles begin to link in a continuous network when $SrTiO_3$/NiO NP concentration reaches 4 weight percent.

A network of charge carriers can travel through the nanoparticles coupled to the PEO/PVA polymers in the films, changing the properties of the material [26–28].

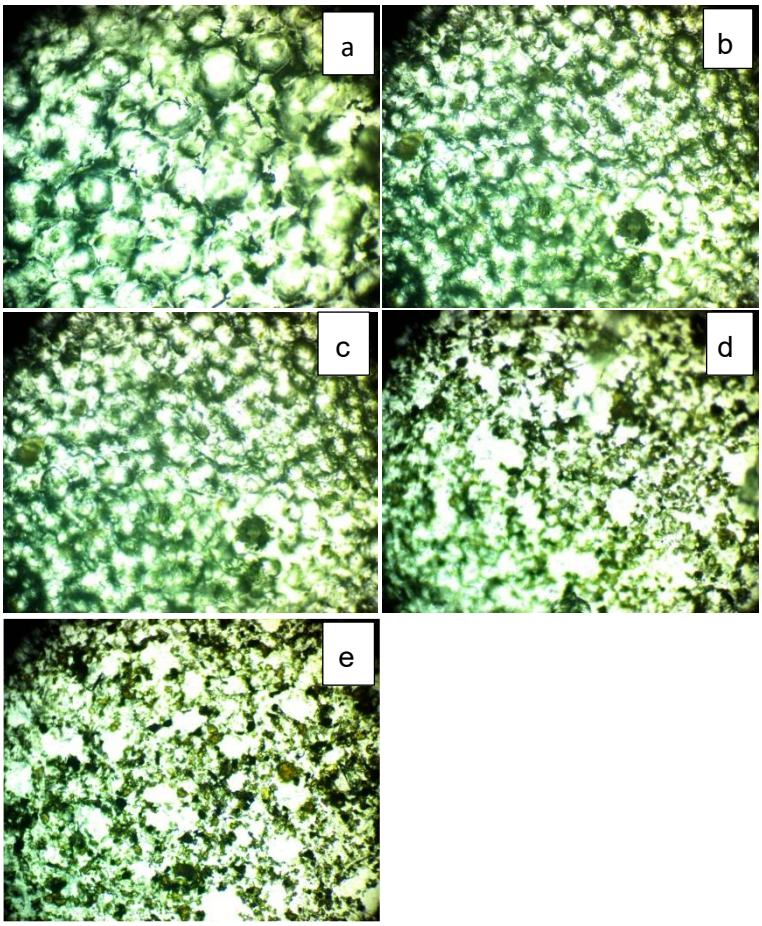

Figure 3. Photomicrographs for PEO/PVA/$SrTiO_3$/NiO nanocomposites at 10× magnification (a) PEO/PVA pure, (b) 1 wt% $SrTiO_3$/NiO, (c) 2 wt% $SrTiO_3$/NiO, (d) 3 wt% $SrTiO_3$/NiO, (e) 4 wt% $SrTiO_3$/NiO.

3.3. Application of PEO/PVA/$SrTiO_3$/NiO nanocomposites for piezoelectric sensors

Figure 4 depicts the parallel capacitance fluctuation for PEO/PVA/$SrTiO_3$/NiO nanocomposites with the pressure for various $SrTiO_3$/NiO nanoparticle concentrations. This figure shows that the capacitance of nanocomposites increases as pressure does [29,30]. The nanocomposite samples include an internal dipole moment. This is called a dipole moment. If there are no forces (electrical or mechanical), the net dipole is in a straight line, as momentum equals zero. As the strain gets bigger, these dipole moments will cause local distributions to change when they are applied to the samples, creating an electric field. Because of this electric field, there are charges above and below the sample [31–33].

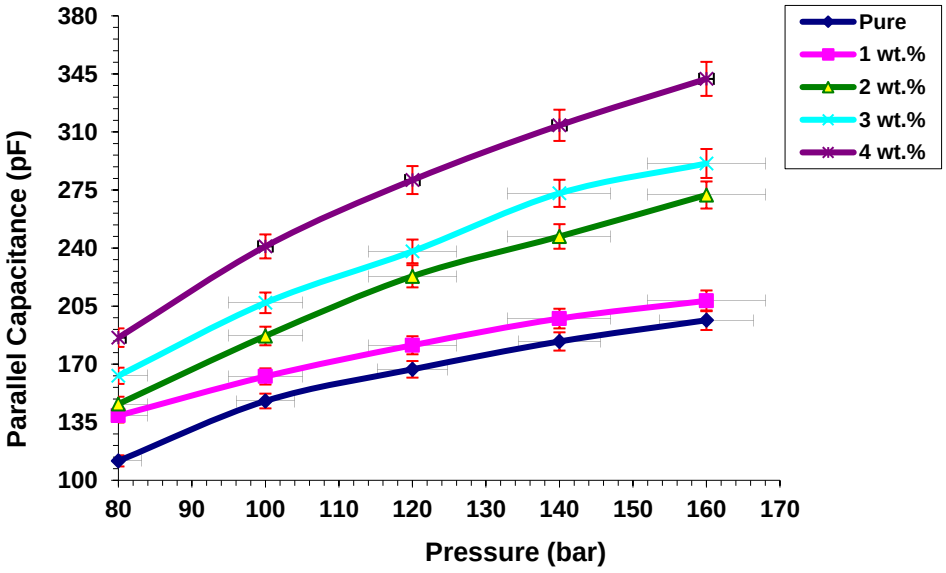

Figure 4. Difference of parallel capacitance for PEO/PVA/$SrTiO_3$/NiO nanocomposites with pressure.

The influence of $SrTiO_3$/NiO nanoparticles on the electrical capacitance (Cp) for PEO/PVA/$SrTiO_3$/NiO NCs is shown in Figure 5 at 80 bars. It is clear from this graph that the electrical capacitance of nanocomposites increases as the concentration of $SrTiO_3$/NiO nanoparticles concentration increases. This might be related to an increase in charge carrier density in nanocomposites [34].

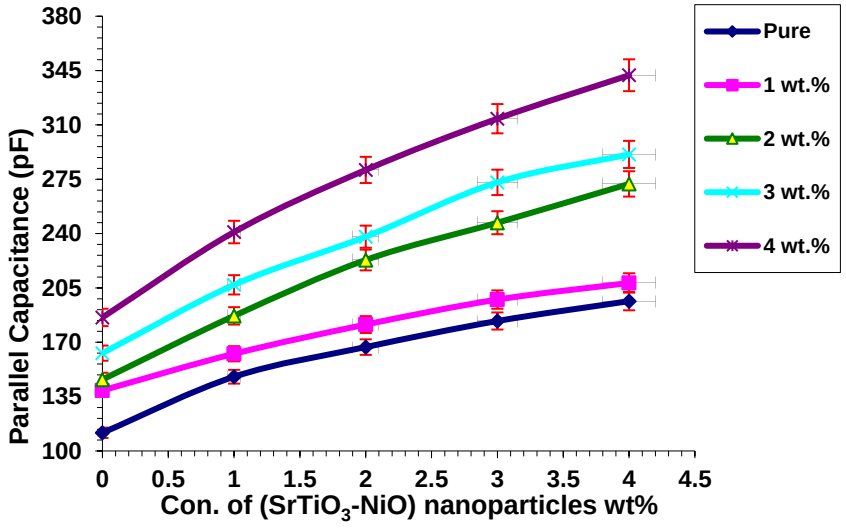

Figure 5. At 80 bar, the influence of $SrTiO_3$/NiO NPs concentration on parallel capacitance is shown for PEO/PVA/$SrTiO_3$/NiO NCs.

The influence of $SrTiO_3$/NiO nanoparticles on sensitivity for PEO/PVA/$SrTiO_3$/NiO NCs is shown in Figure 6. It is clear from this graph that the sensitivity of nanocomposites increases as the

concentration of $SrTiO_3$/NiO nanoparticles concentration increases. This is due to internal dipole moment [35,36].

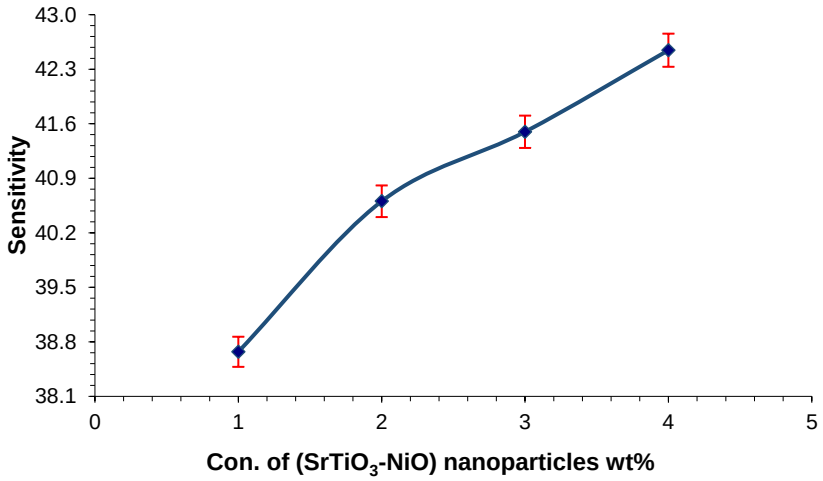

Figure 6. The influence of $SrTiO_3$/NiO NPs concentration on sensitivity for PEO/PVA/$SrTiO_3$/NiO NCs.

3.4. Application of PEO/PVA/$SrTiO_3$/NiO for gamma ray shielding

Fluctuation of (N/N_o) for a mixture of PEO/PVA with various quantities of $SrTiO_3$/NiO nanoparticles is shown in Figure 7. When increasing concentration of $SrTiO_3$/NiO nanoparticles, the transmission radiation decreases. This happens due to an increase in the attenuation radiation [37,38]. Figure 8 shows increasing $Ln(N/N_o)$ of PEO/PVA mixture with increasing $SrTiO_3$/NiO NPs concentrations.

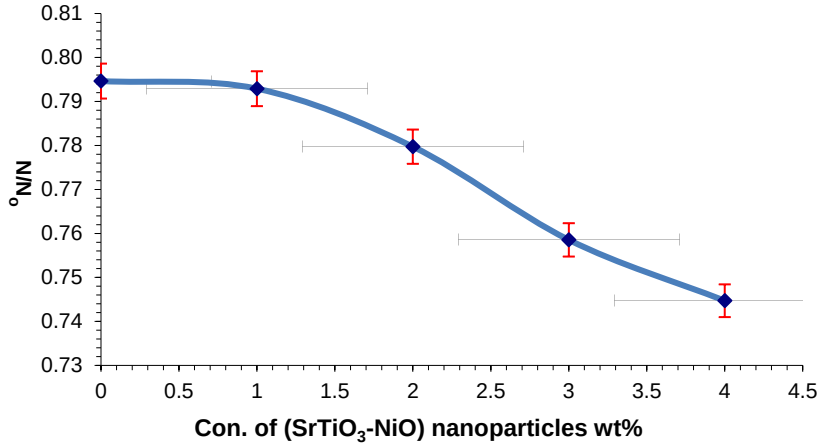

Figure 7. Variance of (N/No) for PEO/PVA mixture with different concentrations of $SrTiO_3$/NiO NPs.

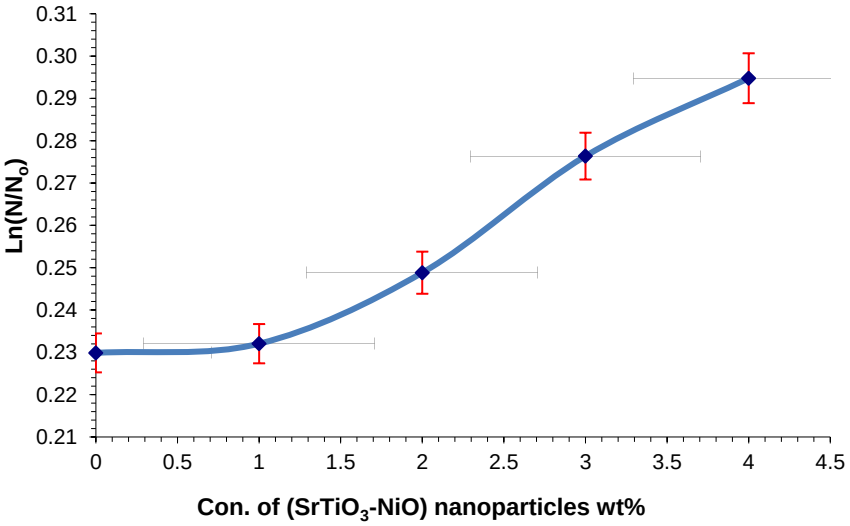

Figure 8. Change of Ln(N/No) for PEO/PVA mixture with different concentrations of $SrTiO_3$/NiO nanoparticles.

Figure 9 shows attenuation coefficient for the PEO/PVA mixture, with varying numbers of $SrTiO_3$/NiO nanoparticles. When the results of polymer nanocomposites and concrete in the figure below were compared, they looked very similar. However, the composite polymer was better than concrete because it was more mobile, had no electrical properties and could prevent neutrons from escaping [39]. The attenuation coefficients rise with increasing $SrTiO_3$/NiO nanoparticles. This is because shielding materials are made of nanocomposites, which either absorb or reflect gamma rays [40–42].

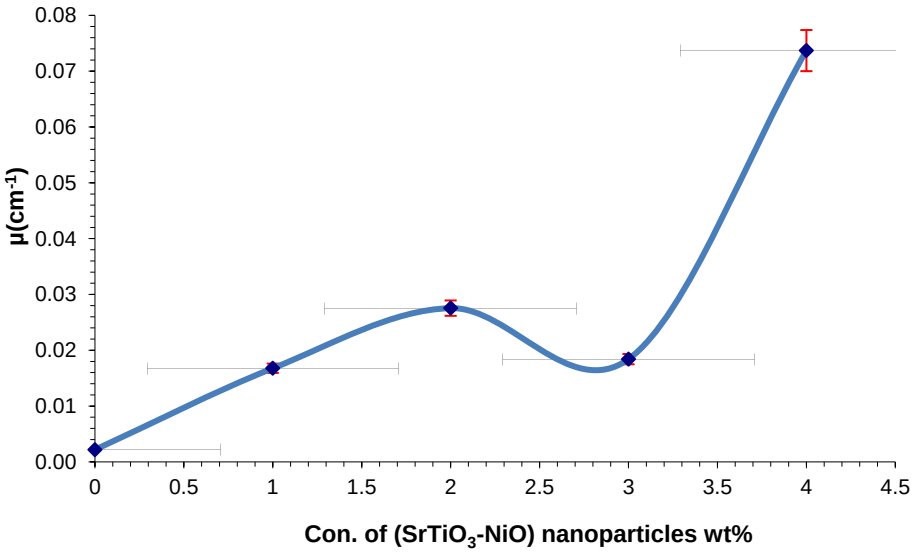

Figure 9. Variance of attenuation coefficients of gamma radiation for PEO/PVA mixture with a different concentration of $SrTiO_3$/NiO nanoparticles.

Figure 10 shows the mass attenuation coefficient (μ/ρ) as a function of concentration of NPs. From this figure, mass attenuation coefficient increases by increasing the concentration of NPs. This is because shielding materials are made of nanocomposites, which either absorb or reflect gamma rays [43,44].

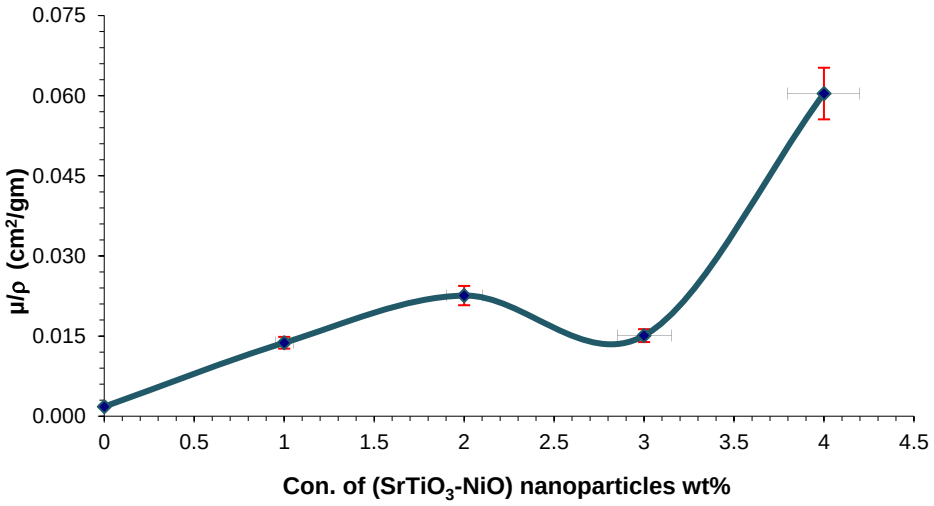

Figure 10. Variation mass attenuation coefficient of PEO/PVA mixture with different concentrations of $SrTiO_3$/NiO nanoparticles.

4. Conclusions

In this study, polymer nanocomposites (NCPs), based on PEO/PVA mixture, were synthesized by means of a solution cast technique. SEM images revealed that the homogenous and coherent surface morphology of the PEO/PVA/$SrTiO_3$/NiO NCs films, pieces or aggregates are dispersed randomly over the top surface. Images captured by an optical microscope revealed that $SrTiO_3$/NiO NPs form a continuous network within the PEO/PVA mixture, and the distribution of $SrTiO_3$/NiO NPs additives was homogeneous in the mixture. The results indicate that when pressure increases, the electrical capacitance of PEO/PVA/$SrTiO_3$/NiO NCs increases. Finally, as the concentration of NPs increases, the attenuation coefficient rises. From these results, it can be concluded that these nanocomposites can be considered as excellent materials for manufacturing low cost, light weight, flexible piezoelectric sensors and gamma ray attenuation.

Acknowledgments

Acknowledgments to University of Babylon.

Conflict of interest

We declare no conflicts of interest.

References

1. Tommasini FJ, Ferreira LdC, Tienne LGP, et al. (2018) Poly(Methyl Methacrylate)-SiC nanocomposites prepared through in situ polymerization. *Mat Res* 21: e20180086. https://doi.org/10.1590/1980-5373-MR-2018-0086
2. Habeeb MA (2011) Effect of rate of deposition on the optical parameters of GaAs films. *Eur J Sci Res* 57: 478–484.
3. Choi B, Park S, Kim S (2015) Preparation of polyethylene oxide composite electrolytes containing imidazoliumcation salt-attached titanium oxides and their conducing behavior. *J Ind Eng Chem* 31: 352–359. https://doi.org/10.1016/j.jiec.2015.07.009
4. Kumar K, Ravi M, Pavani Y, et al. (2012) Electrical conduction mechanism in NaCl completed PEO/PVP polymer blend electrolytes. *J Non-Cryst Solids* 358: 3205–3211. https://doi.org/10.1016/j.jnoncrysol.2012.08.022
5. Mohammed AH, Habeeb MA (2022) CO_2O_3 nanofiller-based polymer blend nanocomposites for enhanced optical properties for optoelectronics devices and as a model of antibacterial. *HIV Nurs* 22: 1167–1172. https://doi.org/10.31838/hiv22.02.225
6. Habeeb MA (2014) Dielectric and optical properties of (PVAc-PEG-Ber) biocomposites. *J Eng Appl Sci* 9: 102–108. https://doi.org/10.36478/jeasci.2014.102.108
7. Dooley KM, Chen SY, Ross JR (1994) Stable nickel-containing catalysts for the oxidative chupling of methane. *J Catal* 145: 402–408. https://doi.org/10.1006/jcat.1994.1050
8. Hosseini MA, Malekie S, Kazemi F (2022) Experimental evaluation of gamma radiation shielding characteristics of Polyvinyl Alcohol/Tungsten oxide composite: A comparison study of micro and nano sizes of the fillers. *Nucl Instrum Methods Phys Res* 1026: 166214. https://doi.org/10.1016/j.nima.2021.166214
9. Hosseini MA, Zareb H, Malekie S (2023) Raman spectroscopy of electron irradiated Multi-Walled Carbon Nanotube for dosimetry purposes. *Radiat Phys Chem* 202: 110535. https://doi.org/10.1016/j.radphyschem.2022.110535
10. Safdari MS, Malekie S, Kashian S, et al. (2022) Introducing a novel beta-ray sensor based on polycarbonate/bismuth oxide nanocomposite. *Sci Rep* 12: 2496. https://doi.org/10.1038/s41598-022-06544-6
11. Ebrahimi N, Hosseini MA, Malekie S (2020) Preliminary study of linearity response of γ-irradiated graphene oxide as a novel dosimeter using the Raman spectroscopy. *Bull Mater Sci* 43: 233. https://doi.org/10.1007/s12034-020-02177-5
12. Zike ZI, Habeeb MA (2022) Role of $BaTiO_3$ /TiO_2 nanofillers on the optical characteristics of biopolymer for optics and photonics fields. *HIV Nurs* 22: 1185–1189. https://doi.org/10.31838/hiv22.02.229
13. Shirinov AV, Schomburg WK (2008) Pressure sensor from a PVDF film. *Sens Actuators A Phys* 142: 48–55. https://doi.org/10.1016/j.sna.2007.04.002
14. Janczak D, Słoma M, Wroblewski G, et al. (2014) Screen-printed resistive pressure sensors containing graphene nanoplatelets and carbon nanotubes. *Sensors* 14: 17304–17312. https://doi.org/10.3390/s140917304
15. Obaid HN, Habeeb MA, Rashid FL, et al. (2013) Thermal energy storage by nanofluids. *J Eng Appl Sci* 8: 143–145. https://doi.org/10.36478/jeasci.2013.143.145

16. Liao YC, Xu DG, Zhang PC (2018) Preparation and characterization of $Bi2O_3$/XNBR flexible films for attenuating gamma rays. *Nucl Sci Tech* 29: 99. https://doi.org/10.1007/s41365-018-0436-7
17. Habeeb MA, Jaber ZS (2022) Enhancement of structural and optical properties of CMC/PAA blend by addition of zirconium carbide nanoparticles for optics and photonics applications. *Eur J Phys* 4: 176–182. https://doi.org/10.26565/2312-4334-2022-4-18
18. Jebur QM, Hashim A, Habeeb MA (2020) Fabrication, structural and optical properties for (Polyvinyl alcohol-polyethylene oxide iron oxide) nanocomposites. *Egypt J Chem* 63: 611–623. https://dx.doi.org/10.21608/ejchem.2019.10197.1669
19. Erdem M, Baykara O, Dogru M, et al. (2010) A novel shielding material prepared from solid waste containing lead for gamma ray. *Radiat Phys Chem* 79: 917–922. https://doi.org/10.1016/j.radphyschem.2010.04.009
20. Mahdi SM (2022) Evaluation of the influence of $SrTiO_3$ and CoO nanofillers on the structural and electrical polymer blend characteristics for electronic devices. *Dig J Nanomater Biostruct* 17: 941–948. https://doi.org/10.15251/DJNB.2022.173.941
21. Habeeb MA, Hashim A, Hayder N (2020) Structural and optical properties of novel (PS-Cr_2O_3/$ZnCoFe_2O_4$) nanocomposites for UV and microwave shielding. *Egypt J Chem* 63: 697–708. https://dx.doi.org/10.21608/ejchem.2019.12439.1774
22. Atta ER, Zakaria KM, Madbouly AM (2015) Study on polymer clay layered nanocomposites as shielding materials for ionizing radiation. *Int J Recent Sci Res* 6: 4263–4269.
23. Abbas NK, Habeeb MA, Algidsawi AJK (2015) Preparation of chloro penta amine cobalit(III) chloride and study of its influence on the structural and some optical properties of polyvinyl acetate. *Int J of Polym Sci* 2015: 926789. https://doi.org/10.1155/2015/926789
24. Hayder N, Habeeb MA, Hashim A (2020) Structural, optical and dielectric properties of (PS-In_2O_3/$ZnCoFe_2O_4$) nanocomposites. *Egypt J Chem* 63: 577–592. https://doi.org/10.21608/ejchem.2019.14646.18874
25. Mahdi SM, Habeeb MA (2022) Synthesis and augmented optical characteristics of PEO-PVA-$SrTiO_3$-NiO hybrid nanocomposites for optoelectronics and antibacterial applications. *Opt Quantum Electron* 54: 854. https://doi.org/10.1007/s11082-022-04267-6
26. Chandra K, Ipsita C, Debdulal S, et al. (2015) Modified clad optical fibre coated with PVA/TiO_2 nanocomposite for humidity sensing application. *Int J Smart Sens Intell Syst* 8: 1424–1442. https://doi.org/10.21307/ijssis-2017-813
27. Jebur QM, Hashim A, Habeeb MA (2020) Structural, AC electrical and optical properties of (polyvinyl alcohol-polyethylene oxide-aluminum oxide) nanocomposites for piezoelectric devices. *Egypt J Chem* 63: 719–734. https://dx.doi.org/10.21608/ejchem.2019.14847.1900
28. Habeeb MA, Hashim A, Hayder N (2020) Fabrication of (PS-Cr_2O_3/$ZnCoFe_2O_4$) nanocomposites and studying their dielectric and fluorescence properties for IR sensors. *Egypt J Chem* 63: 709–717. https://dx.doi.org/10.21608/ejchem.2019.13333
29. Habeeb MA, Abdul Hamza RS (2018) Novel of (biopolymer blend-MgO) nanocomposites: Fabrication and characterization for humidity sensors. *J Bionanosci* 12: 328–335. https://doi.org/10.1166/jbns.2018.1535
30. George FF, Leon MC, Ayo A, et al. (2010) Metal oxide semi-conductor gas sensors in environmental monitoring. *J Sens* 10: 5469–5502. https://doi.org/10.3390/s100605469

31. Habeeb MA, Kadhim WK (2014) Study the optical properties of (PVA-PVAC-Ti) nanocomposites. *J Eng Appl Sci* 9: 109–113. https://doi.org/10.36478/jeasci.2014.109.113
32. Narsimha P, Shilpa J, Syed K, et al. (2006) Electrical and humidity sensing properties of polyaniline/WO_3 composites. *Sens Actuators B Chem* 114: 599–603. https://doi.org/10.1016/j.snb.2005.06.057
33. Geng WC, Li N, Li XT, et al. (2007) Effect of polymerization time on the humidity sensing properties of polypyrrole. *Sens Actuators B Chem* 125: 114–119. https://doi.org/10.1016/j.snb.2007.01.041
34. Hadi AH, Habeeb MA (2021) Effect of CdS nanoparticles on the optical properties of (PVA-PVP) blends. *J Mech Eng Res Developments* 44: 265–274. https//jmerd.net/03-2021-265-274
35. Roy MK, Mahloniya RG, Bajpai J, et al. (2012) Spectroscopic and morphological evaluation of gamma radiation irradiated polypyrole based nanocomposites. *J Adv Mater Lett* 3: 426–432. https://doi.org/10.5185/amlett.2012.6373
36. Akkurt I, Akyıldırım H, Mavi B, et al. (2010) Gamma-ray shielding properties of concrete including barite at different energies. *Prog Nucl Energy* 52: 620–623. https://doi.org/10.1016/j.pnucene.2010.04.006
37. Habeeb MA, Mahdi WS (2019) Characterization of (CMC-PVP-Fe_2O_3) nanocomposites for gamma shielding application. *Int J Emerging Trends Eng Res* 7: 247–255. https://doi.org/10.30534/ijeter/2019/06792019
38. Habeeb MA, Hamza RSA (2018) Synthesis of (Polymer blend-MgO) nanocomposites and studying electrical properties for piezoelectric application. *Indones J Electr Eng Inf* 6: 428–435. https://doi.org/10.11591/ijeei.v6i1.511
39. Kaur S, Singh KJ (2013) Comparative study of lead borate and lead silicate glass systems doped with aluminum oxide as gamma-ray shielding materials. *Int J Innov Technol Explor Eng* 25: 172–175.
40. Hashim A, Habeeb MA, Jebur QM (2019) Structural, dielectric and optical properties for (Polyvinyl alcohol-polyethylene oxide manganese oxide) nanocomposites. *Egypt J Chem* 63: 735–749. https://dx.doi.org/10.21608/ejchem.2019.14849.1901
41. Zhang J, Yu J, Jaroniec M, et al. (2012) Noble metal-free reduced graphene oxide-$Zn_xCd_{1-x}S$ nanocomposite with enhanced solar photocatalytic H_2-production performance. *Nano Lett* 12: 4584–4589. https://doi.org/10.1021/nl301831h
42. Hadi AH, Habeeb MA (2021) The dielectric properties of (PVA-PVP-CdS) nanocomposites for gamma shielding applications. *J Phys Conf Ser* 1973: 012063. https://doi.org/10.1088/1742-6596/1973/1/012063
43. Mahdi SM, Habeeb MA (2022) Fabrication and tailored structural and dielectric characteristics of ($SrTiO_3$/NiO) nanostructure doped (PEO/PVA) polymeric blend for electronics fields. *Phys Chem Solid State* 23: 785–792. https://doi.org/10.15330/pcss.23.4.785-792
44. Mehrara R, Malekie S, Kotahi SMS, et al. (2021) Introducing a novel low energy gamma ray shield utilizing Polycarbonate Bismuth Oxide composite. *Sci Rep* 11: 10614. https://doi.org/10.1038/s41598-021-89773-5

AIMS Press